DOI: 10.13009/EUCASS2023-764
Aerospace Europe Conference 2023 – 10TH EUCASS – 9TH CEAS

Optimization of Wave-Plasma Interaction in RF Powered Propulsion Technology based on Ultra-Compact Helicon Reactor

Theodora ANDREESCU [1], Simona DANESCU [2], Alexandru CANCESCU [3], Dan IFRIM [4]*
** Corresponding author*
1 COMOTI Launchers and In-Space Advanced Propulsion, 061126 Bucharest, Romania,
theodora.andreescu@comoti.ro
2 COMOTI Launchers and In-Space Advanced Propulsion, 061126 Bucharest, Romania,
simona.danescu@comoti.ro
3 COMOTI Launchers and In-Space Advanced Propulsion, 061126 Bucharest, Romania,
alexandru.cancescu@comoti.ro
4 COMOTI Launchers and In-Space Advanced Propulsion, 061126 Bucharest, Romania,
dan.ifrim@comoti.ro

Abstract

The emergence of new space business models imposes a high level of competitiveness driven by reliability, performance, cost, and flexibility for the electric propulsion systems. Relevant strategic applications such as Earth Observation under 250 km (VLEO), Space Exploration, Telecommunication, Human Spaceflight require innovative propulsion technologies able to generate a certain thrust level at high specific impulse during an extended operational time, while being compact, light, and efficient. To overcome the drawbacks related to the most mature electric propulsion technology such as IEs or HETs, COMOTI and ESA in the framework of the GSTP De-Risk Program explored the potential of a disruptive RF Powered Propulsion Technology based on helicon discharges with the strategic goal to advance the development of a new cost-effective generation of Space Transportation System. Based on this, a family of ultra-compact Helicon Plasma Thrusters can be derived, enabling new space market such as large constellation in LEO-MEO and air-breathing satellites in VLEO.

The Helicon Plasma Thruster couples a radiofrequency magnetized cylindrical plasma source based on multipole magnetic confinement system and a magnetic nozzle acceleration stage. The current prototype is composed of a discharge chamber where plasma is generated, an m=+1 mode RF antenna and a magnetic nozzle. The RF power is transferred to the antenna through a RF Generator and a Matching Box that adapts the RF power to the plasma electromagnetic behavior. In the thruster`s first stage a cold and dense argon plasma is generated through a stochastic RF - electron interaction at a representative frequency of 13.56 MHz. To provide the required environment for both excitation of the propagating electromagnetic wave and for radial plasma confinement in the helicon reactor, it is involved a multipole magnetic confinement system based on a set of 8 plate-shape NdFeB permanent magnets displace in alternating rows of north and south pole along the confinement tube.

This scientific paper is devoted to study the coupled effect of the m=+1 half-wavelength Right Helical Antenna and Nagoya Type III and of the static magnetic field intensity on power absorption in the first stage of the HPT. In order to maximize the power deposited into the helicon reactor, several m=+1 RF antennas of different architectures and lengths have been tested in relevant laboratory conditions in both Continuous Wave Mode and Pulsed Wave Mode within $50 \div 500 W$ power range. It is demonstrated that half-wavelength Right Helical Antenna produces non-axisymmetric RF energy coupling, which generates higher electron density than the Nagoya Type III antennas. Since the propulsive matrix is related to the wave-plasma coupling by the RF antenna, the actual combined numerical-experimental research improved the prediction/assessment of a high argon plasma density within the HPT. Alongside, this study summarizes the various performance parameters of the propulsion system along a discussion of ongoing research and future roadmap.

DOI: 10.13009/EUCASS2023-764

1. Introduction

To overcome the weaknesses of current in-space propulsion systems, such as the hallow cathode neutralizers, high voltages acceleration grids and limited propellants [1][2], innovative concepts need to be developed to meet the requirements of future missions. Emerging technologies such as electrode- less plasma thrusters can prospectively eliminate many of the design and manufacturing issues encountered to date, leading to higher reliability, throttlability, longer operational lifetime, lower development, and recurring costs.

To align with the market's needs, COMOTI and ESA, in the framework of GSTP De-Risk Program, explored the potential of a disruptive RF Powered Propulsion Technology based on helicon discharges with the strategic goal to advance the development of a new cost-effective generation of Space Transportation System. The experimental achievements relate that the Helicon Plasma Thruster has a great potential to address new space markets, increasing the Technology Readiness Level up to a flight qualification process. Based on this, multiple space mission scenarios can be identified: low-power constellation flight in LEO-MEO, air-breathing satellites in Very Low Orbits, GEO platforms, Space-tugs market, and scientific deep space missions. Each of these missions presents different requirements, but the versatility of this RF Propulsion Technology could potentially increase performances. Versatile in terms of propellants, it may operate both with unconventional propellant (iodine) and molecular gasses such as CO_2, O_2, H_2O, this technology can be used as Atmosphere – Breathing Electric Propulsion System (ABEP) for drag compensation of VLEO comsats and EO satellites. The strategic goal behind extending the VLEO missions is to develop an advanced commercial and economic model of Earth observation systems. Recent studies have explored the benefits of operation in VLEO compared to altitudes of above 500 km. With decreasing altitude, the resolution of optical instruments increases. Advanced Concepts such as Variable Specific Impulse Magnetoplasma Rocket (VASIMR, $\sim 200kW, \sim 5.8N$) [4][2][19] and others Helicon Double Layer Thruster –HDLT ($\sim 1kW, \sim 11mN$) [4][5], Mini –helicon Plasma Thruster ($\sim 1kW, \sim 11mN$) [19] are in various stage of development and field test, offering a great promise for the future of space exploration.

An optimized design of an ultra-compact Helicon Plasma Thruster requires a deep comprehension of wave-plasma coupling mechanism alongside a synergistic correlation between the propulsion metrics and plasma parameters. A generic of the derived requirements for the Helicon Plasma Thruster is provided below:

- Thruster's class: 10 mN – 500 W,
- Target specific impulse: $1000 - 1500$ s;
- RF frequency: 13.56 MHz;
- Power envelops: 8-600W to evaluate the mode transition (capacitive – inductive – helicon);
- Plasma density: up to 10^{12}cm^{-3};
- Argon mass flow rate: 6-50 sccm;
- Testing pressure: $2 \cdot 10^{-5}$ mbar.

Helicon reactors of high electron density n_e, leading to high thrust force, but a low electron temperature T_e, reducing inner discharge wall damages, are mandatory for future space transportation systems. [14] To solve a problem of the electrode erosion, a high-density helicon reactor with Magnetic Nozzle (MN) acceleration is promising in a fully electrodeless propulsion system. Since the electrodes have no direct contact with plasma in the system, it is expected to have a longer operational lifetime.

In this paper it is presented the development and experimental characterization of an ultra-compact Helicon Plasma Thruster based on multipole magnetic confinement system and m=+1 mode antenna, named HEMIS. Having a fully cathode - less and gridles architecture, it is expected to provide a longer operational lifetime, greater reliability and a significant reduction in the cost and complexity of the propulsion system compared to space heritage technologies. The dispersion relation for the helicon wave in a cylinder was derived for designing a plasma source that allows the propagation of helicon waves. Two types of m=+1 mode RF antennas are proposed from power deposition consideration, half-wavelength Right Helical and Nagoya Type III, of different lengths. RF Sources can typically operate in three modes: Capacitive, Inductive and Helicon, depending on the source parameters and antenna geometry. [5] The transition between these modes is analyzed alongside the power deposition profiles (Helicon-Trivelpiece Gould Mode conversion). [10]

2. Helicon Plasma Thruster Architecture

This cutting – edge technology is designed as a low-cost solution to impact the market`s needs in terms of lifetime limitations, compatibility with a wide broad of propellants and scalability in terms of size and power, that are prominent among the established technologies in use today.

DOI: 10.13009/EUCASS2023-764

The full concept of the HEMIS prototype (Figure 1) embodies the properties of multipole magnetic system. Two of these magnetic structures are connected into a continuous multistage plasma reactor, where each stage serves a unique purpose. In the first stage, cold and dense argon plasma is produced through helicon wave's excitation. An essential peculiarity of its operation is the resonance excitation of helicon waves (or whistler wave) which is long scale electromagnetic waves in the range of ion cyclotron frequency and electron cyclotron frequency ($\omega \ll \omega_{ce}$), known as high–frequency compression Alfven wave or low-frequency whistler. [13] [18]

Helicon Plasma Thruster is composed of a cylindrical discharge chamber where plasma is generated, an RF antenna wrapped around the discharge tube and a magnetic nozzle. The RF power is supplied to the antenna thanks to the RF subsystem, consisting of an RF wave generator and a Matching Network that adapts the RF power to the plasma electromagnetic behavior. In addition, a feeding system is attached to the back of the chamber. Also, a set of magnets surrounding the discharge tube generates the required magnetic field inside the discharge region and the plasma expansion area, forming a magnetic nozzle topology. The magnetic system involved in the HEMIS thruster design is based on permanent magnets. It is designed to allow excitation of the propagating electromagnetic waves, ensure radial confinement, and accelerate plasma in the magnetic nozzle at supersonic speeds. To provide the required environment for RF wave deposition in the Helicon Reactor, it is involved a multipole magnetic confinement system based on a set of 8 plate-shape NdFeB permanent magnets of 38EH grade displaced in alternating rows of north and south pole along the confinement tube, with an inward magnetization in the radial direction.

An improvement of HPT propulsion metrics could be attained by a proper design of the magnetic nozzle and a large thrust could be achieved by increasing electron pressure. Therefore, ring-shaped NdFeB magnet, displaced at the confinement tube exit, will create a rapidly converging-diverging magnetic nozzle. The design purpose of the thruster acceleration stage is to approach an operation with no radial plasma losses to the wall and from the magnetic nozzle. For the acceleration stage (magnetic nozzle structure), a ring-shaped NdFeB magnet, gold plated of 38EH grade, is placed near the confinement tube exit. The assembled system consists of a $300\,mm$ diameter quartz tube closed at one end with a custom polyamide injector plate. The multipole configuration provides an approximately axial magnetic field inside the confinement tube of up to 400G.

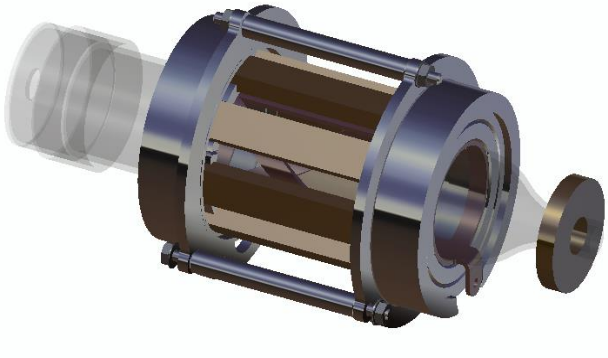

Figure 1: 3D Model of the HEMIS - Ultra-compact Helicon Plasma Thruster

3. The Effects of Key Parameters on Power Absorption

A volume-averaged model of a RF Powered Propulsion Technology is proposed as starting point in design procedure. The neutral argon is injected into the helicon reactor at a fixed rate and a plasma is generated by circulating a RF current in a $m = +1$ antenna, where m represents the azimuthal mode number. The global model, based on energy and particle balance equations, predicts four variables in the thrusters' discharge chamber: the electron temperature, the plasma density, the neutral gas density (atom) and neutral gas temperature. [14] [18]

The dispersion relation for a uniform plasma is derived from the low-frequency whistler waves: [16]

$$\omega = \frac{k k_{\parallel} B_0}{e n_0 \mu_0} \tag{1}$$

Within an ultra-compact helicon reactor, the square root of the total wave number k^2 is the sum of $k_{\perp}^2$ and $k_{\parallel}^2$, where $k_{\parallel}/k$ is $cos\theta$ and the finite value of $k_{\perp}$ is set by the boundary conditions. For a discharge chamber of radius a aligned with B, the lowest radial mode has $k_{\perp}$ approximately equal to p_{11}/a, where $p_{11} = 3.83$ is the first zero of

DOI: 10.13009/EUCASS2023-764

the Bessel function $J_1(\boldsymbol{k}_\perp \boldsymbol{r})$. A simplified version of Eq. (1) by neglecting electron inertia and assuming uniform plasma density, provides the dispersion relation in terms of experimental parameters: [7]

$$k = \frac{\omega}{k_\parallel}\frac{\omega_p^2}{\omega_c c^2} = e\mu_0 v_p\left(\frac{n_0}{B}\right) \approx \frac{3.83}{a}, \tag{2}$$

with $v_p = \omega/k_\parallel$ the wave's phase velocity along the tube. The above equation shows that the helicon resonance requires $n_0 a/B$ to be a constant. For each given radius a, the density should vary linearly with B; and for given n_0, the required field B should vary linearly with tube radius a. [6]

A possible methodology for improving HPT performance is to manipulate the power conditioning of RF input. Involving pulsed power operation allows the thrusters to release itself from the normal limitation stemming from 0D power balance.[18] This enables better plasma properties and high electron temperature. Both Continuous Wave Mode (CWM) and Pulsed Wave Mode (PWM) power conditioning have been used to generate thrust. [7] When part of the gas is ionized, the ions are accelerated by the pre-sheath electric field with the Bohm velocity. Therefore, the ion reaches the wall at a higher speed than the thermal speed of the neutral gas. When it hits the wall, the ion recombines to become a neutral gas, and this neutral either gets pumped out or slowly diffused back toward the center at the thermal speed. Because the neutral can reach the pump faster in the presence of plasma, the neutral pressure in the discharge chamber reaches a steady state during RF pulses. [8]

This advanced space propulsion concept involves complex physics such as wave-plasma coupling, cross-field diffusion and plasma acceleration and detachment from MN field lines.The global model of particle and power balance was involved to support the thruster design as well as to deduce plasma parameters dependency on different operating conditions. The Global Model developed by Liberman and Lichtenberg allows the determination of plasma density, plasma potential and electron temperature and consists of two balance equation: particle and power balance. The first equation predicts electron temperature, being determined by equating the total surface particle loss to the total volume ionization.

The ion particle balance is related by: [18]

$$\Im\frac{dn_e}{dt} = K_{iz}n_e n_g \Im - n_e u_B\big(h_R(2\pi R_s L_s) + h_{BW}(\pi R_s^2) + h_T(\pi R^2)\big), \tag{3}$$

with:
n_e, n_g −plasma and neutral densities.

The first term on the right denotes the ion generation rate, with K_{iz} the ionization rate constant and $\Im$ is the effective volume of the helicon discharge chamber. The second term on the right stands for the ion loss rate where $u_B = \sqrt{kT_e/m_i}$ the Bohn velocity is and R_s, L_s are the reactor radius and length. The h_R, h_{BW} and h_T are the sheath edge-to-centre density ratios for the radial walls, back wall and exit plane.
On the other hand, the neutral particle balance equation is as follow: [18]

$$\Im\frac{dn_g}{dt} = \frac{\dot{m}}{m_i} + n_e u_B\big(h_R(2\pi R_s L_s) + h_{BW}(\pi R_s^2)\big) - n_g(\pi R^2)\frac{V_t}{4} - K_{iz}n_e n_g \Im \tag{4}$$

In the Eq. (4), the first term accounts for the propellant distributed to the discharge chamber with $\dot{m}$ the propellant mass flow rate and m_i the ion mass. The second term accounts for the neutral particles achieved through ion recombination on the radial and back walls of the plasma reactor. The last term on the right accounts for neutral particles lost to diffusion at the exit with $V_t = \sqrt{8k_B T_g/\pi m_i}$ the average thermal speed. The last term represents the neutral lost to ionization collisions.

The power balance is: [18] [7]

$$P_{abs}(t) = \frac{d}{dt}\left(\frac{3}{2}en_e T_e\right)\Im + P_c + P_i + P_e + P_{e,t}, \tag{5}$$

where P_{abs} is the power absorbed by the plasma electrons. The terms, $P_c, P_i, P_e, P_{e,t}$ are the power lost to electron-neutral collisions, ion kinetic energy at the sheath edge, electron energy at the radial and back wall sheath edges and the electron energy lost in the MN. [19]

$$P_c = en_e n_g V_{eff}(K_{iz}\mathcal{E}_{iz} + ex\mathcal{E}_{ex}) \tag{6}$$

DOI: 10.13009/EUCASS2023-764

$$P_i = e\frac{1}{2}T_e n_e u_B\left(h_R(2\pi R_s L_s) + h_{BW}(\pi R_s^2) + h_T(\pi R^2)\right) \tag{7}$$

$$P_e = e(V_s + 2T_e)n_e u_B\left(h_R(2\pi R_s L_s) + h_{BW}(\pi R_s^2)\right) \tag{8}$$

$$P_{e,T} = e\left(2T_e + \frac{1}{2}M_{det}^2 T_e\right)n_e u_B(h_T \pi R^2) \tag{9}$$

with:
$\mathcal{E}_{iz}, \mathcal{E}_{ex}$- ionization and excitation energies for Argon
$V_s = \frac{T_e}{2} ln\frac{m_i}{2\pi m_e}$ −sheath potential
M_{det} −ion Mach number at the MN point where ions detach from the magnetic field lines

The central plasma density n_0 results from energy balance by equating the total absorbed power to the total power lost: [15]

$$n_0 = \frac{P_{abs}}{e u_B A_{eff} \mathcal{E}_T} \tag{10}$$

In Eq. 10, A_{eff} is the effective particle loss area defined by $A_{eff} = 2\pi R_S^2 h_L + 2\pi R_S L_S h_R$. When axial magnetic field is $400G$, by using the expected plasma density of $\sim 2.4 \cdot 10^{13} cm^{-3}$ and the RF frequency of $13.56\ MHz$, the axial wavelength comes out to be $\lambda_z \sim 15.64\ cm$.

The RF antenna has been designed to provide a maximum wave–plasma coupling, having the wavelength $\lambda_z = 2L_a$. [4]

$$L_a = \lambda_z/2 \tag{11}$$

As part of our modular test program, we are assessing two antenna design: half-wavelength Right Helicon and Nagoya Type III (Figure 2). The nominal antenna length was found to be **7.8 cm**, determining the axial wavenumber and the rotational symmetries.

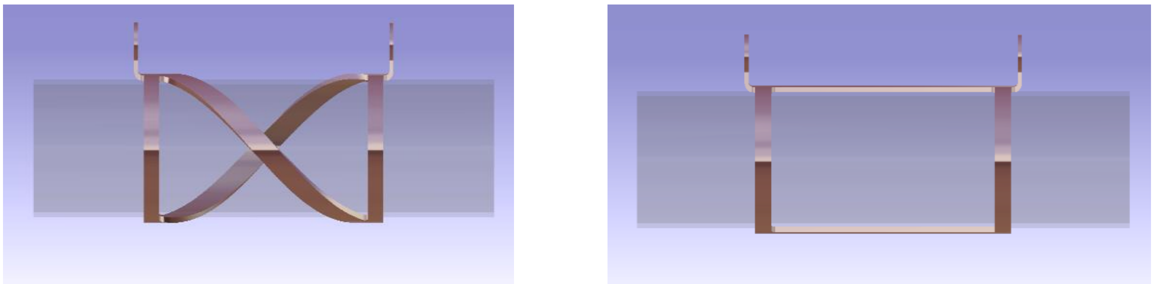

a) b)

Figure 2: m=+1 mode antennas a) Half-wavelength Right Helicon, b) Nagoya Type III

The efficiency of the antenna can be viewed as the plasma-wave interaction. The current of the horizontal legs, parallel to the applied magnetic field has a big impact on plasma-interaction optimization. The vertical legs on the other hand provide a return path. Since the antenna length is smaller compared to free-space wavelength of the RF signal, the current pattern is fixed nearly instantly. The rising magnetic field induces a divergent – free electric field (E_{em}) in the plasma. Since the antenna has a finite $k_\parallel$, E_{em} reverses sign periodically in the z direction, building up a space charge pattern. [9] [11] The space charge develops a curl-free electric field (E_{es}), developing until the total electric field parallel to B. For an $m = +1$ configuration, these currents and space charges are of opposite polarity on the top and bottom of the plasma. Since the electrostatic field has its source in internal space charges it ultimately couples to the electromagnetic field of the helicon wave. [13]

The two types of waves existing in this frequency range are helicon (H) waves and electrostatic Trivelpiece – Gould (TG) waves. The dispersion relations for these waves are: [7] [17]

DOI: 10.13009/EUCASS2023-764

$$\omega_H = \omega_c \frac{k_\parallel k_t c^2}{\omega_p^2} \tag{12}$$

$$\omega_{TG} = \omega_c \frac{k_\parallel}{k_t} \tag{13}$$

Due to the sharp coupling with azimuthal currents of the RF antenna, the helicon (H) waves are directly excited, whilst TG waves are not able to be excited due to a weak coupling effect. On the other hand, the TG waves are generated in the plasma through a specific surface mode conversion mechanism. One a wave is excited in the plasma, the radial RF current related to the electron oscillations must vanish at the edge side of the plasma. Electron current on the magnetic field is a sum of $E \times B$ drift in the wave electric field **E,** and the magnetic field **B** and of the polarization drift. The helicon waves have circularly polarized eigenmodes with electric field varying as $E(r)exp[i(m\theta + kz - \omega t)]$. When the wavefield varies as $exp(-i\omega t)$, the amplitude of the radial current is: [13]

$$j_r = -\frac{\omega_p^2}{4\pi\omega_c}\left(E_\theta + i\frac{\omega}{\omega_c}E_r\right), \tag{14}$$

with

E_r −radial electric field
E_θ −azimuthal electric field

The right-hand part of the Eq. (14) cannot be zero with a single helicon wave, resulting in a generation of the TG wave at the plasma boundary. The radial wavelength of the TG wave is ω_c/ω times shorter than the axial one and thereby, helicon waves excited by an external antenna in a space propulsion system generate short-scale and intensive TG excitation. It appears that the TG wave absorbs most if the energy from the H wave, therefore forming a main channel for RF power absorption. As generated near plasma edge, the TH wave transfer energy into the plasma and deposits it by collisions. In contrast to the H wave, the TG wave is strongly damped by collisions. Its depth of penetration into the plasma, $\delta_{TG} = k_\parallel^{-1}(\omega^2/\upsilon)$, decays with rising collision frequency ν and magnetic field. At a fixed collision frequency, these two regimes are divided by a magnetic field, with a strength provided by the following relationship: [7] [17] [19]

$$B_{H-TG} = 5.7 \cdot 10^{-8}\frac{\omega^2}{\nu}\frac{1}{k_\parallel r_p} \quad (G) \tag{15}$$

At a low applied magnetic field, below B_{H-TG} the mechanism of power absorption is focused in the core while at high field, above B_{H-TG} it turns out to be on the surface. For a low-aspect-ratio helicon reactor (low length-to-radius ration L/R_r) it is useful to consider the fields as discrete superpositions of different standing waves. [19] All these harmonics in the plasma are a combination of the H wave excited directly by the antenna and the TG wave due to the surface mode conversion. Because the RF energy is absorbed in the reactor through TG of these harmonics, the overall power absorption falls if one of the harmonics achieves the antiresonance.

4. The discharge characteristics of ultra-compact helicon reactors

Three distinctive modes of operation of the helicon plasma thruster are distinguished by the structure of the plasma-wave field. Based on the electron heating mechanism, an ultra-compact helicon reactor can operate in the capacitively coupled mode (E-mode), inductive coupled mode (H-mode) and helicon-wave coupled mode (W-mode), being in synergistic correlation with the RF supply power, driving frequency and magnetic field strength. The most convenient regime for energy deposition inside the helicon reactor is the double-wave one, where long-wavelength helicon waves and short-wavelength, quasi-perpendicular TG waves can propagate. In the high frequency regime, $\sqrt{\omega_{ce}\omega_{ci}} < \omega < \omega_{ce}$, hybrid resonances are not valid, and the density limit occurs due to the coalescence of the helicon and Trivelpiece – Gould (TG) waves. [9]

In this research projects, two types of helicon plasma sources have been investigated. One is a confined helicon reactor having half-wavelength Right Helical antenna and the other having Nagoya Type III antenna. Based

DOI: 10.13009/EUCASS2023-764

on this, four different breadboards have been manufactured and validated in vacuum environment having different antenna geometry and lengths (78mm, 87mm and 65mm). For simplicity, in this paper it was decided to present the commissioning and the validation procedure of the best HEMIS breadboard.

a)

b)

Figure 3: a) Half –wavelength Right Helical Antenna of 65mm, 78mm and 87mm, b) Nagoya Type III Antenna of 65mm, 78mm and 87mm

The HEMIS prototype consists of 30mm outer radii discharge chamber closed at one end with a custom ceramic injection plate, an exhaust section of 10mm, a m=+1 mode RF Antenna (half-wavelength Right Helical) of 78 mm length and 1.25 mm thickness, wrapped along with the discharge chamber, a multipole magnetic confinement system composed of 8 plate-shape NeFeB 38EH grade permanent magnets with gold plating (70mm length, 10 mm width and 5 mm thickness. In the plasma production stage, the energy coupled to the plasma is stored in the electron temperature energy. The plasma acceleration stage comprises a ring-shaped NdFeB 38EH grade permanent magnet disposed in the throat section.

Figure 4: Experimental Set-Up

The experimental testing facility was developed to validate the physics breakthrough of an ultra – compact helicon reactor for space applications. Several characteristic features have been investigated such as helicon-wave coupling, surface mode conversion, neutral depletion, and magnetic nozzle effects. The plasma was generated in $13.56\ MHz$, delivered as ms pulses or in CW operation. The peak power available is $600\ kW$. Also, the RF is matched to the Nagoya Type III and half-wavelength Right Helical with a variable capacitor L-type Matching Network. The aim of this study is to characterize the relationship between the design parameters and the performance parameters. Figure 4 presents a schematic diagram of the HEMIS experimental testing facility together with the associated pulsing circuit and control electronics. The RF output of the reactor is modulated by a signal from a RF Generator (Coaxial Power –RFG600-13) controlled by a computer running a LabView programme. The L-type Matching Network (AMN600) ensures that the impedance of the antenna and helicon reactor is matched to that of RF Generator to maximize the forward power and to minimize the reflected power.

DOI: 10.13009/EUCASS2023-764

The profile and the amplitude of the pulse signal can be programmed, but the actual shape of the RF pulse envelope is imposed by the characteristics of the RF Generator and its associated load. For pulse operation the matching network is adjusted manually to provide a minimum average reflected power. The reactor discharge was ignited by different m=+1 mode types antennas, such as Nagoya Type III and half-wavelength Right Helical configuration. Also, the AMN 600 Matching Box consists of two variable capacitors, the load capacitor (C_L) and tune capacitor (C_T) which can be manually tuned if the matching is not optimum in the automatch mode. The RF Generator can supply RF power up to $600\ W$ and has a maximum reflection power limit of $90W$ and an inbuilt output standard resistance of $50\ \Omega$. The propellant flow is regulated by a flow controller (Brinkhorst EL-FLOW F-201CV model) mounted outside the vacuum chamber. Other ports of the space simulation chamber provide access for thermal evaluation by IFR cameras and emission spectra. The vacuum chamber has a pumping system consisting of a multi-stage Roots pump, air-cooled; with a maximum pumping speed of $28\,\mathrm{m}^3/\mathrm{h}$(Pfeiffer-ACP-28-40 model) and a turbomolecular pump (Pfeiffer HiPace 400 with TC400 Turbo Pump Controller). A valve with a manual actuator is installed between the mechanical pump and the turbomolecular pump top to prevent back-flow. The pumping system supports a base pressure of less than$2 \cdot 10^{-5}$ mbar. The chamber pressure is monitored using a Pfeiffer gauge TPG 361.

5. Experimental Testing Campaign

The RF generator provides 600 W at 13.56 MHz, operating in both Continuous Wave Mode (CWM) and Pulsed Wave Mode (PWM), allowing for cooling of antenna and of the matching network. The experimental testing campaign has been performed in two ways: either in Continuous Wave mode (CW Mode) or Pulsed Power mode. For both ways, the flow rate was varied between 0 and 50 sccm.

For the continuous mode, the gas is inserted at an initial rate of 5 sccm (the minimum value allowed by the flowmeter), and plasma is turned on at a value of 100 to 150 W. Depending on the tuning in the matching box, the value of the reflected power is lowered manually by using the keys on the matching box controller. As the reflected power is kept low, the gas rate is slowly increased to about 20 sccm, and the forwarded power is also increased to 250 to 300 W. This allows for heat to build up in the entire system (cables, thruster). This heating up allows further tuning of the reflected power up to a point where it gets negligible (10-20W) for higher power input. During this time, the gas flow is lowered to the best value for low reflected and high forwarded power values. The regular operation in the continuous wave is performed for up to 30 minutes, while spectra are acquired and photography and filming are performed.

For all tested configurations, the magnetic field along the axis of the confinement tube was obtained with NdFeB magnets, with the magnetization vector parallel to the symmetric axis, place above the chamber to have the requested value of the magnetic field at the antenna. The measured magnetic field inside the helicon reactor was 40mT (400G).

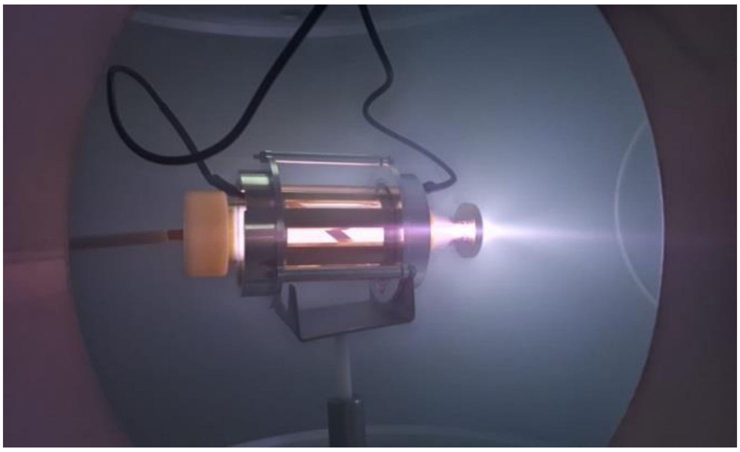

Figure 5: Photographs of Experimental Hardware in CW Mode at 200 W P_{wd} and 60 W P_{ref} at 8 sccm of Argon

To facilitate a pulse mode regime, we have developed a software routine that automatically drives the RF power and gas flow to follow the pattern in the Figure 6. The duty cycle includes an Off Timer (toff), during which both RF and gas are off (or set to a low value), an On Timer (ton) during which both RF and gas are on (or set to a high value) simultaneously, and a delay (tdelay) between turning gas and RF on, as seen in the picture.

DOI: 10.13009/EUCASS2023-764

This test sequence gives us a fundamental understanding of mechanism governing processes, helping to design an optimal helicon reactor and to find a proper modulation period. The possibility of controlling the reaction inside the plasma source by changing the modulation period was also underlined by adjusting the auto-ignition parameters. In the first stage of power application during the ON-TIME, the electron temperature increases rapidly above the steady-state value. More charged particles are trapped inside the plasma production stage of the thruster due to the relatively higher power applied that for the continuous wave (CW). In the first stage of the OFF TIME, the electron temperature drops quickly, resulting in smaller particle loss (Bohm) velocity. Therefore, it was observed a higher time – average power. The time evolution of the electron temperature and the plasma density could be calculated by solving the particle and energy balance equations. It was found that much higher plasma densities can be achieved by selecting an appropriate modulation period than when operating with Continuous Wave (CW).

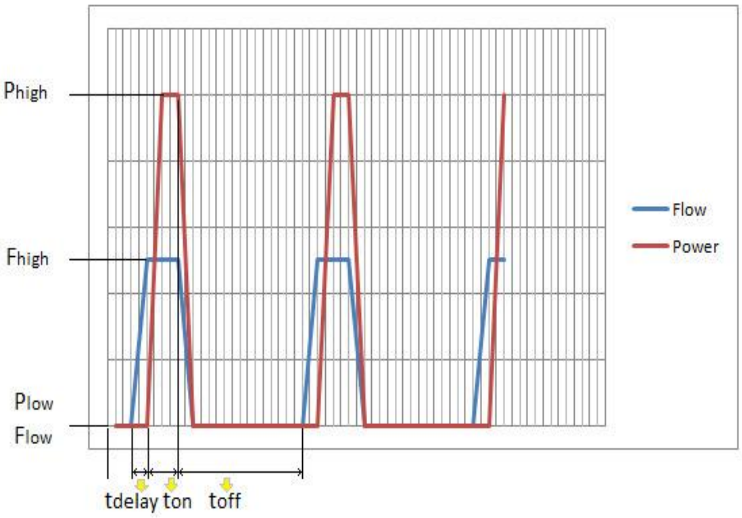

Figure: 6 Auto Ignition Pulse Mode regime

The pulsed mode starts with the same pressure value as above. However, the gas insertion is performed simultaneously as the RF power and shut off according to the pulse scheme. This allows the gas to enter the thruster tube and create a moment of higher pressure inside, which, correlated with the RF pulse, ignites the plasma far more efficiently and easily than the continuous mode. For example, values of 600 W are obtained for the forward power (with 30 to 50 W of reflected power), which cannot be obtained in continuous mode. Flow rates are like the continuous mode, with values of 5 to 40 sccm. The pulse parameters (length of RF pulse, length of gas flow, delay between gas flow and RF pulses, time between pulses, RF value and gas flow value) can be varied better to tune the reflected power and aspect of the discharge. The most used experimental values are RF pulse ON – 0.5 sec, GAS flow On – 1 sec, Delay – 0 sec, the time between pulses of 1 to 2 seconds. RF power values were selected between 200 and 600 W, while gas flow rates between 5 and 50 sccm. During the experiments, the spectra acquisition is performed by accumulations of 40 data sets with exposure times of 400 ms, that is, for 16 seconds, allowing for a good signal on the final data.

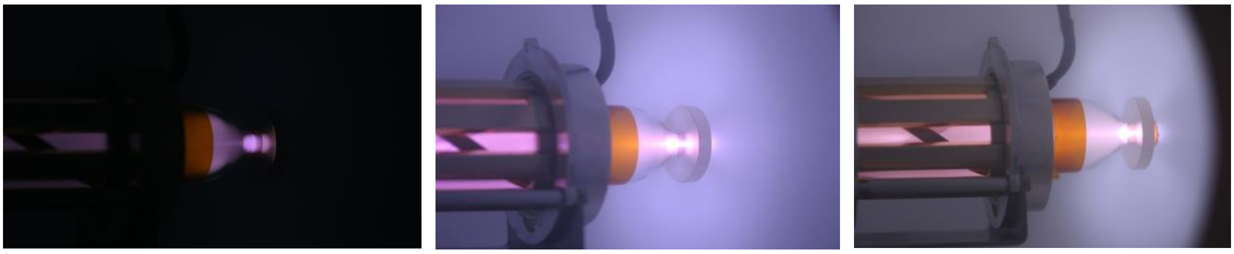

Figure: 7 Photographs with nominal configuration of the Experimental Hardware in High Power Pulsed Wave Mode (500 W with 60 W reflected power)

The RF output and the Argon flow rate was modulated by a signal from the RF Generator controlled by a PC running a LabView programme. The same computer controls the Data Acquisition System, the Spectrograph and the Flow Controller. The profile, amplitude of the analogue pulse signal can be programmed, but the actual shape of

DOI: 10.13009/EUCASS2023-764

the RF pulse envelope is determined by the characteristics of the RF Generator and its load. For this pulse operation, the Matching Box is adjusted manually to provide a minimum average reflected power.

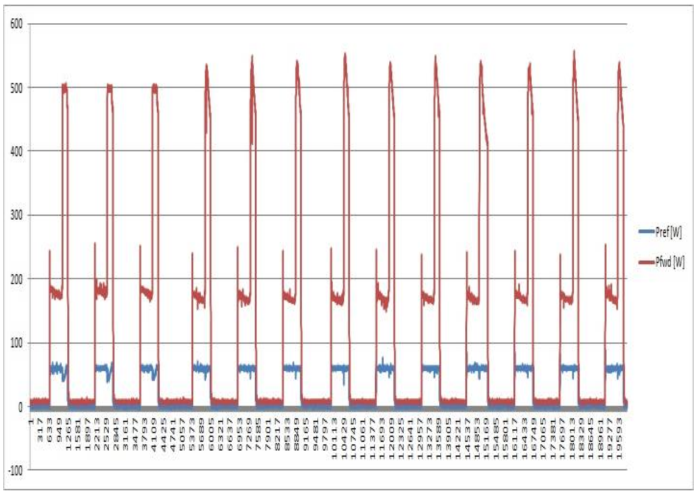

Figure:8 The variation of the P_{ref} and P_{fwd} during a Pulsed Mode cycle

The pulsed mode is required to operate at higher RF power values, as the heat build-up would otherwise destroy the device in continuous wave. Also, the gas bubble created by inserting the gas in pulses allows for better plasma ignition and matching. The configuration of the thruster quart tube, with a higher diameter at the antenna level and much smaller diameter near the nozzle, combined with the gas bubble resulted from the pulsed mode of operation, constricts the generated plasma inside the nozzle far better compared to the continuous mode; this translates into a closer to higher pressure plasma generation and behavior, and better collimation of the exiting plasma jet. It has been observed that the plasma performances have been significantly modified by pulsing the discharge. For a range of gas pressures and power levels in pulsed plasmas, the time-average electron temperature and average ion loss rate from the plasma is reduced. As a result, a higher average ion density can be achieved than for continuous mode plasma having the same geometrical and operational parameters.

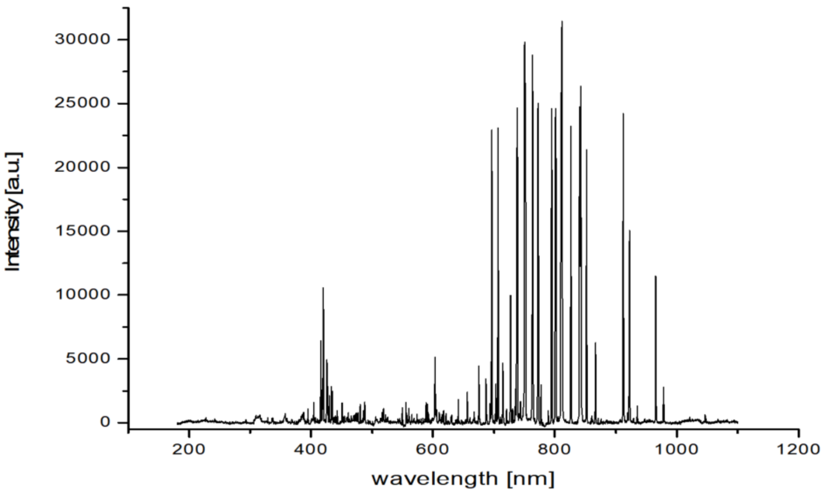

Figure 9: Discharge spectrum for the 78 mm Right Helical Antenna, for 500W, 60 W Reflected Power, 12 sccm, 1 sec ON

The emission spectra for the laboratory Helicon Plasma Thruster model have been performed for various operational parameters, with the main goal to provide a qualitative understanding of the plasma ionization. The plasma inside the source is almost impossible to access with intrusive diagnostics because they will perturb the plasma. The gain information about the plasma inside the HEMIS prototype non-intrusive diagnostics has been used. The spectral

DOI: 10.13009/EUCASS2023-764

measurements performed allow determining the plasma density and electron temperature for various operational parameters such as RF Power, Argon flow rates and applied external magnetic field.

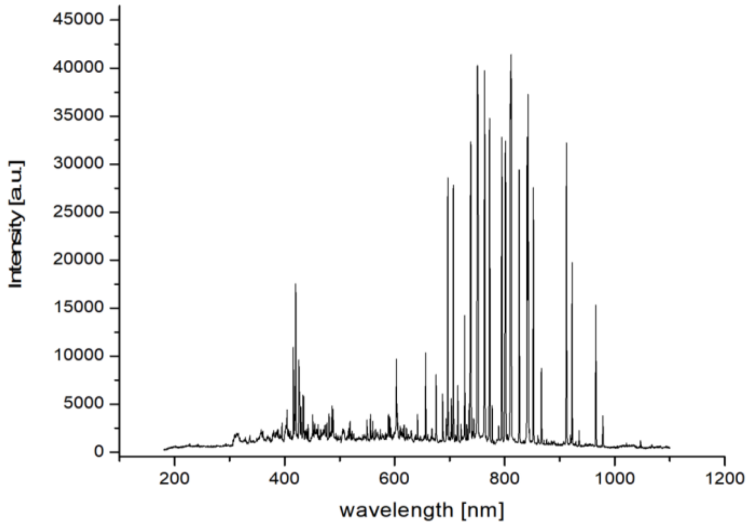

Figure 10: Discharge spectrum for the 78 mm Right Helical Antenna, for 300W, 60 W Reflected Power, 12 sccm, 1 sec ON

Spectra acquired with our set-up identified the presence of Argon neutrals and ions as well as derived information about excited states. The two main forms of argon have been identified Ar-1 (neutrals) and Ar-II, the single ionised ions. An AvantesAvaSpec Dual-Channel-ULS4096CL-EVO-UA-10 (200-1100 wavelength range, 0.05-20nm resolution) was used. A laptop was interfaced with the optical fibre (200 μm core diameter). A dedicated calibration lamp has been also used.

For the diagnosis of the helicon plasma, a program was used to simulate the spectral intensity of the Argon red lines based on the radiative collisional model. This model considers the populations of 21 levels: 1st1 the fundamental level (denoted by 1), 1s5, 1s3 metastable level, 1s4, 1s2 resonant levels, 2p1 -2p10 levels, 2sd3, 3p, and hl (high levels) each grouped into a single level, the Argon excimer population Ar^{2*} and the ion population Ar^{+} and Ar^{2+}. Since the spectral velocities are partially absorbed in the plasma (the plasma is optically thick for this), it was necessary to calculate the *escape factor*. This escape factor, which ultimately affects both the line intensities and the population in the lines, requires some knowledge of the discharge gas temperature, pressure, path through the plasma, and the distribution of the particles along this path. The estimated plasma density and electronic temperature for the 300 W RF Supply Power in Pulsed mode for the Right Helical Antenna of 78 mm length were:$n_0 = 5 \cdot 10^{17} m^{-3}$, $T_e = 5\ eV$. Obtained HEMIS thruster parameters in optimal operating point are: mass flow rate 12sccm, RF power 300W, thrust $F = 3.21 mN$, specific impulse $\mathrm{I_{sp}} = 1128$ s.

6. Conclusions

Most plasma thrusters encounter electrode damage, leading to limited mobility in space. Therefore, applications in deep space exploration and VLEO Earth Observation are limited. To solve a problem of the electrode erosion, a high-density helicon reactor with MN acceleration is promising in a fully electrodeless propulsion system. In this paper it was presented the theoretical background along with the development procedure and experimental validation of the HEMIS-Helicon Plasma Thruster proof-of-concept. The strategy behind the development was to create a flexible test platform which allows the exploration of a wide range of relevant control variables (discharge chamber geometry, mass flow rate, magnetic topology, antenna type and geometry, RF Supply Power, relative displacement between components) to aid in understanding the efficiency and utilization problems that affect this device, test the limits of the HPT and identify points for improvement for an optimal design.

Helicon plasma proves abrupt jump between low- and high-density modes, being stimulated by a continuous variation of external parameters, such as RF supply power. These densities jump are associated with transitions between three modes of antenna-to-plasma coupling: capacitive, inductive and wave (helicon) coupled modes. A Capacitive Coupling (CC) to Inductive Couple (IC) mode transition is intrinsic for any inductive discharge, whereas a transition between IC and WC is a representative feature of the helicon discharge.

DOI: 10.13009/EUCASS2023-764

The thruster has been experimentally evaluated with success in high vacuum environment in the 50-500W RF Power range and 8-50sccm of argon flow rate at 13.56MHz both in Continuous and Pulsed Wave modes. Based on plasma-wave coupling analysis a set of scaling laws is proposed to underline a synergistic relationship between geometry and operational parameters. The guidelines for further HPT optimization are underlined to get a full image of the argon plasma structure within both the source and the magnetic nozzle.

References

[1] Gilland, J. and N. Hershkowitz. 1998. Application of a helicon discharge to electric propulsion. *In: 34th AIAA Joint Propulsion Conference*, Vol. 3934, 1998.

[2] Mario, M., and N. Jaume. 2015. Design and development of a $1kW$ – class helicon antenna thruster. *In: Joint Conference of 30th ISTS, 34th IECP and 6th NSAT, Hyogo-Kobe, Japan July 4-10.*

[3] Trezzolani, F., and A.L. Fabrs. 2013. Low Power Radio-Frequency Plasma Thruster Development and Testing.In *33th International Electric Propulsion Conference*, No. IECP-2013-153.

[4] Tian, B., and E.Ahedo. 2014. Assessment of helicon plasmas thruster technology for space missions, *Space Propulsion Conference,* European Space Agency.

[5] Isayama, S., S. Shinohara, T. Hada and S.H. Chen. 2019. Spatio-temporal behavior of density jumps and the effect of neutral depletion in high-density helicon plasma. *Physics of Plasmas.* doi: 10.1063/1.5093920

[6] Francis, F. Chen. 2015. Helicon discharges and sources: a review. *Plasma Sources Sci. Technol.24 -014001*

[7] Shogo, I., S.Shinohara and T.Hada. 2018. Review of Helicon High-Density Plasma: Production Mechanism and Plasma/Wave. *Plasma and Fusion Research.* Volume 13, 1101014.

[8] Gilland, J., R. Breun and N. Hershkowitz. 1998. Neutral pumping in a helicon discharge. *Plasma Source Sci. Technol*. 7 416-422.

[9] Chang, L., and H. Xinyue. 2018. Coupling of RF Antennas to Large Volume Helicon Plasma. *AIP Advances:* 8 045016.

[10] Ronald, L., and J. Mark. 2001. Wave propagation and power deposition in magnetically enhanced inductively coupled helicon plasma sources. *Journal of Vacuum Science&Technology* 19,76.

[11] Konstantin, P. and V.B. Taranov.1996. Volume and surface rf power absorption in a helicon plasma source. *Plasma Sources Sci. Technol.5*: 474-491.

[12] Lehane,J.A., P.C. Thonemann.1965. An experimental study of helicon wave propagation in a gaseous plasma. In: *Proc.Phys.Soc.,* Vol.85.

[13] Isayama, S., S. Shinohara, and T.Hada. 2018. Review of Helicon High-Density Plasma: Production Mechanism and Plasma/Wave Characteristics. *J.Plasma and Fusion Research*. Volume 13, 1101014.

[14] Coppola, G., M.Panelli and F. Battista. 2023. Preliminary design of helicon plasma thruster by means of particle swarm optimization. *J. AIP Advances.* 13, 055209.

[15] Lafleur, T. 2014. Helicon plasma thruster discharge model. *J. Physics of Plasmas 21.* 043507.

[16] Igor, A. Kotelnikov. 2014. On the density limit in the helicon plasma sources. *J. Physics of Plasmas.*21, 122101.

[17] Shinohara, S., D. Kuwahara, Y. Ishiami and S. Nakanishi. 2020. Extremely small-diameter, high – density, radio-frequency, plasma sources and central gas feeding for next-generation eletrodeless plasma thrusters. *J. Review of Scientific Instruments*. 91, 073507.

[18] Michael, A.L., L.Allon. 2005. Principles of Plasma Discharges and Materials Processing, Second Edition. Wiley Interscience ISBN 0-471-72001-1.

[19] Shunjiro, S., Y.Kawai. 1995. Estimation of Electric Fields from Magnetic Field Distributions and an Application to Helicon Wave. *J. Appl. Phys.Vol.34*.